



72nd Conference of the Italian Thermal Machines Engineering Association, ATI2017, 6-8 September 2017, Lecce, Italy

Development of a virtual calibration methodology for a downsized SI engine by using advanced valve strategies

Teodosio Luigi^{a,*}, Tufano Daniela^a, Bozza Fabio^a

^aIndustrial Engineering Department, University of Naples "Federico II", Via Claudio 21, 80125 Naples, Italy

Abstract

The calibration phase of a new engine at test bench is an expensive and time-consuming process. To support the engine development process, in this paper a numerical methodology aiming to define the optimal control parameters is proposed for a downsized VVA SI engine. First, a 1D engine model is build-up in GT-Power and is enhanced with phenomenological sub-models. 1D model is then validated against the experimental findings, at high- and part-load operations.

In a second stage, a numerical calibration strategy is defined, to automatically identify, for various engine loads/speeds, the control parameters, ensuring optimal performance and complying with proper system limitations.

Complete engine maps are computed for different control strategies (*EIVC* and *Throttled*). An application example is also presented, where computed maps are embedded in a vehicle model to predict the CO₂ emission produced along a NEDC cycle.

© 2017 The Authors. Published by Elsevier Ltd.

Peer-review under responsibility of the scientific committee of the 72nd Conference of the Italian Thermal Machines Engineering Association

Keywords: SI engine; Virtual calibration; 1D model; Control Strategies; Vehicle Simulation.

Nomenclature

Acronyms

1D/3D one/three dimensional

* Corresponding author. Tel.: +39-081-7683285; fax: +39-081-2394165.

E-mail address: luigi.teodosio@unina.it

A/F	air-to-fuel ratio
BMEP	Brake mean effective pressure
BSFC	Brake specific fuel consumption
CAD	Crank angle degree/Computer aided design
DoE	Design of Experiment
ECU	Electronic control unit
EIVC	Early intake valve closure
ICE	Internal Combustion engine
IVC	Intake valve closure
MFB ₅₀	50% of Mass fraction burned
MSE	Mean squared error
NEDC	New European Driving cycle
PFI	Port Fuel Injection
PID	Proportional Integral Derivative Controller
SA	Spark Advance
THR	Throttle
TIT	Turbine Inlet Temperature
VVA	Variable Valve Actuation system
VVT	Variable Valve Timings
WG	Waste-gate
WOT	Wide Open throttle

Symbols

A_L	Flame front laminar area
A_T	Flame front turbulent area
c_{d3}	Fractal dimension multiplier
D_3	Flame front fractal dimension
L_{Gib}	Gibson length scale
L_{max}	Flame wrinkling maximum scale
L_{min}	Flame wrinkling minimum scale
m_b	Burned mass
S_L	Laminar flame speed
t	Time

Greeks

ρ_u	Density of the unburned gas
σ	Mean squared error

1. Introduction

The calibration phase of a modern spark ignition engine consists into the identification, for different operating points, of the optimal values for control parameters (including spark timing, air-to-fuel ratio, valve strategy, turbocharger setting, etc.) with the aim to reach proper targets such as maximum power/torque, minimum fuel consumption, and minimum pollutants and noise emissions. In addition, some operative constraints (maximum levels of in-cylinder pressure, boost level, exhaust temperature, turbocharger speed, knock absence, etc.) have to be respected to ensure engine and sub-components safety.

Modern engine architecture shows a large number of degrees of freedom, and each control parameter has to be varied around a presumed set point for a predefined operating condition. From a practical point of view, a reduced set

of optimal engine calibrations at test bench is identified once assigned the desired performance targets and operating constraints. This task is usually realized through the adoption of Design of Experiment (DoE) methodologies [1]. However, in this case the experimental calibration is an expensive and time-consuming process when an adequate resolution in terms of engine speed and load levels is required.

In the light of the above consideration, an engine pre-calibration through numerical models would be very helpful for engine manufacturers, in order to reduce development costs and time. In the current literature, some examples of model-based calibration methodologies for internal combustion engines (ICEs) are available. Among different modeling approaches, 1D models showed the capability to describe the entire engine, and to predict the performance parameters in the whole operating plane, thanks to a reduced computational effort. Consequently, a 1D model represents the unique numerical approach capable to perform a virtual engine calibration. Of course, model accuracy has to be preliminary proven in a wide range of operating conditions.

As an example, Grasreiner et al. [2] studied the numerical calibration of a turbocharged direct-injection SI engine with Variable Valve Timing (VVT), utilizing a 1D model for gas exchange calculations. This approach was enhanced with quasi-dimensional (QD) models for in-cylinder turbulence (k - ϵ) and combustion (eddy burn-up model) and was then validated with air-charge and burn rate measurements in different load/speed points. Acceptable accuracy in the prediction of combustion results across the engine map was obtained, too. The integrated models were utilized to define ECU functions of in-cylinder peak, crankshaft torque and exhaust gas temperature.

Bozza et al. [3] followed a different approach by coupling a 1D model to an external optimizer (modeFRONTIERTM), with the aim to search the calibration strategy minimizing the fuel consumption at part load of a turbocharged VVA SI engine. The adopted optimization approach, based on a genetic algorithm, reproduced the experimentally identified calibration corresponding to the numerically derived Pareto frontier in BMEP-BSFC plane. Even if the above discussed technique represents a very advanced approach for calibration studies, it involves longer development phase and high computational efforts to perform a wide exploration of the engine map.

In this paper, a virtual calibration methodology is presented, based solely on a refined 1D model. The modeling approach followed here makes use of advanced phenomenological sub-models allowing for a physically based reproduction of the turbulence, combustion and knock phenomena. The calibration procedure is fully automatized and validated over a wide range of operating conditions and different control strategies. Furthermore, the adopted technique shows the advantage to explore the entire engine map with reduced computational time.

The calibration procedure is applied to a small-size Port Fuel Injection (PFI) turbocharged in-line twin-cylinder engine, whose main characteristics are listed in Table 1. In particular, this engine is equipped with a Valve Variable Actuation (VVA) module, capable to control the intake valve lift profile. A preliminary experimental analysis is carried out at manufacturer test bench where both high and part loads are investigated at different speeds and valve strategies.

First, a 1D model of the whole engine is developed in GT-Power framework and widely validated against experimental findings, showing high accuracy. In a second stage, a numerical calibration strategy is proposed to build up the whole engine performance map for two different engine control strategies: a classic throttle based approach (labelled as *Throttled*) and an early intake valve closure strategy (labelled as *EIVC*). The developed calibration procedure is also validated through the comparison of numerically derived control parameters and the standard manufacturer calibration at the test bench. Finally, computed fuel maps are embedded in a vehicle model to quantify the potential reduction in CO₂ emission, over a driving cycle, of the *EIVC* approach with respect to the *Throttled* one.

Table 1. Engine main features

Engine architecture	SI PFI VVA Turbocharged Twin-cylinder
Compression ratio and Layout	10; 4 valves/cylinder
Displaced Volume, cm ³	875.4
Bore x Stroke, and Connecting rod length, mm	80.5 x 86, 136.85
Maximum brake power, kW	63.7@5500 rpm
Maximum brake torque, Nm	146.7@2000 rpm

2. Models description and validation

A 1D model of the examined engine is developed in GT-Power environment. In particular, it is coupled to phenomenological “in-house developed” sub-models to accurately reproduce the in-cylinder processes, including turbulence, combustion, knock, and heat transfer. They are implemented into the code under the form of “user routines”. Referring to the combustion process, a two-zone (burned and unburned gases) “fractal” approach [4], [5] is adopted, to directly predict the burning rate, as a function of combustion chamber geometry, engine operating parameters and valve strategies. According to the fractal formulation, the burning rate is proportional to the turbulent flame area, A_T , as reported by eq. (1):

$$\frac{dm_b}{dt} = \rho_u A_T S_L = \rho_u A_L S_L \frac{A_T}{A_L} = \rho_u A_L S_L \left(\frac{L_{\max}}{L_{Gib}} \right)^{D_3 - 2} \left(\frac{L_{Gib}}{L_{\min}} \right)^{(D_3 - 2) \cdot c_{d3}} \quad (1)$$

ρ_u being the unburned gas density, A_L the area of the laminar flame front, and S_L the laminar flame speed. The latter is evaluated by an empirical correlation according to the thermodynamic state, equivalence ratio and charge dilution [6]. A_L is, indeed, derived by an automatic procedure implemented in a CAD software, processing the actual 3D geometry of the combustion chamber. As known, the turbulent flame front can be correlated to the laminar flame one through the wrinkling factor, A_T/A_L . An extension of the conventional “fractal” combustion model [7] is here considered, where the flame front is wrinkled with a reduced extent, or even is not affected by the turbulent eddies showing a characteristic length scale smaller than the Gibson scale, L_{Gib} . In eq. (1) L_{\max} and L_{\min} are the length scales of the maximum and minimum flame wrinkling, respectively; D_3 the fractal dimension, and c_{d3} represents a tuning constant. If the latter constant is equal to 1, a standard fractal formulation [8] is obtained, while a reduced wrinkling of the smaller eddies is introduced with c_{d3} lower than 1.

A phenomenological $K-k$ turbulence sub-model is employed to properly estimate the wrinkling factor. It describes the time-evolution of the turbulent and mean kinetic energies along the whole engine cycle [3]. Actually, the above sub-model takes directly into account both the selected control strategy (*EIVC* and *Throttled*) and the operating conditions (speed and load). Turbulence and combustion sub-models are properly tuned [3] and a single set of tuning constants has been assigned in the whole engine operating plane.

Referring to the knock modeling, the auto-ignition of the unburned gas is directly described by solving a kinetic scheme for the oxidation of a three-component fuel (iso-octane, n-heptane and toluene) in the unburned zone. In particular, the kinetic scheme here adopted was developed by Andrae et al.[9] and includes 5 elements, 138 species and 633 reactions. Knock event is recognized in the model as a sudden jump in the end-gas temperature, due to auto-ignition occurrence. The knock intensity is computed as the pressure increase occurring in an isochoric combustion of the unburned fraction at the knock event [10]. A modified Hohenberg correlation is adopted for heat transfer modeling, while the piston, cylinder liner and head temperatures are calculated by the simplified finite element approach, implemented in GT-PowerTM software.

Concerning the model validation, 284 operating points, including part and high loads, are investigated. At this step, the manufacturer calibration for each control parameter, namely the combustion phasing (MFB_{50}), and the A/F ratio, are imposed in the calculations. Concerning the VVA setting, the Intake Valve Closure (IVC) is specified for *EIVC* control strategy, while the full-lift valve profile is assigned for the *Throttled* one. Depending on the load level, a PID controller selects the waste-gate (WG) and throttle (THR) valves openings to match the experimental BMEP level.

In Fig. 1, the numerical/experimental comparisons in terms of in-cylinder peak pressure (a), BSFC (b), and Turbine Inlet Temperature (TIT) (c) are shown. The figure collects both *EIVC* and *Throttled* operating conditions, plotted in red and black colors, respectively. A good correlation with experimental data is found for the in-cylinder peak pressure, presenting a Mean Squared Error (MSE) of 1.61 bar, while the BSFC shows a higher MSE of 8.64 g/kWh, depending on the concurrent effects of both flow, combustion and heat transfer modeling.

TIT presents a systematic underestimation of about 50°C. The above disagreement is probably due to an inadequate modelling of heat transfer in the exhaust pipes or errors in the measured TIT levels. However, most of the computed results are included in the considered allowable error band $\pm 5\%$, confirming the good capability of the model to predict the whole operating plane.

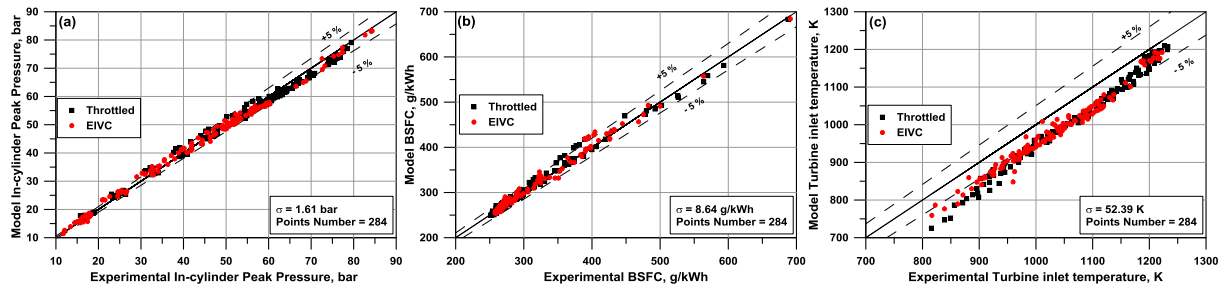


Fig. 1. Experimental vs Model In-cylinder peak pressure (a), BSFC (b), and turbine inlet temperature (c)

3. Virtual Engine Calibration: set-up, validation and results

The validated model is employed to define a numerical procedure to predict the engine performance over its whole operating plane at various control strategies. To this aim, each engine control parameter, namely Spark Advance (SA), WG opening, A/F ratio, throttle (THR) opening, and VVA setting, has to be properly identified. Strategy substantially depends on the specific operating point and, in each case, it has to comply with a number of constraints to limit thermal and mechanical stresses of the engine and its subcomponents. Maximum allowable levels imposed for some parameters are reported below, together with additional limitations:

- Maximum TIT: 930 °C; Maximum in-cylinder peak pressure: 85 bar; Maximum boost pressure: 2.4 bar;
- Optimal combustion phasing: $MFB_{50-opt} = 7.5$ CAD AFTDC;
- Target plenum pressure: 0.88 bar; Knock threshold level: 0.6 bar * rpm/1000.

More details about the above listed specification are reported in [11]. Referring to the more complex *EIVC* control strategy, the calibration procedure is summarized by the listed steps:

- 1) At each engine speed, a preliminary run is performed in the so-called Base-Boost (BB) operation, to select the IVC realizing the maximum volumetric efficiency (IVC_{BB}). The related load level ($BMEP_{BB}$) is also saved and utilized in subsequent steps. In this phase, THR and WG valves are fully opened.
- 2) A second analysis is realized to identify the full load curve. The calculation starts with IVC fixed at IVC_{BB} . Then, the WG valve is slowly closed until the boost pressure reaches the prescribed maximum level (2.4 bar). If required, the boost is reduced to comply with surge margin derived from the compressor map [12]. In addition, during the run, the MFB_{50} is delayed until the predicted knock level is below the prescribed threshold, while a further PID controller reduces the A/F ratio, if the TIT overcomes the maximum allowable level.
- 3) A complete engine plane is computed, covering the entire speed and load range. For each speed, the entire load range is divided in 3 regions, identified by the previously computed $BMEP_{BB}$ and IVC_{BB} :
 - a. Low load range: the prescribed BMEP is reached reducing the IVC below IVC_{BB} , while the THR valve is modified to reach the target plenum pressure. The latter is specified to limit the gas-dynamic noise emission arising when the THR is fully opened.
 - b. Medium load range: the prescribed BMEP is reached by THR opening, while IVC is set to IVC_{BB} . This load range ends at $BMEP_{BB}$, with a fully opened THR.
 - c. High load range: the prescribed BMEP is reached by WG closing, while IVC is set to IVC_{BB} and THR valve is fully opened.
 For each load/speed point, MFB_{50} and A/F ratio are controlled to avoid knock and to respect the TIT limitation, as described in step 2).

For the simpler *Throttled* strategy, the step 1) is still executed with IVC fixed to the full-lift profile to identify the $BMEP_{BB}$ load level. The load range in step 3) is now only split in low-load and high-load regions, where the THR and WG valves are respectively utilized to follow the prescribed BMEP level. The above discussed calibration strategies, fully automatized in a single “subassembly” in GT-Power, require a proper validation, to ensure that optimal BSFC performance are attained all over the operating plane. To this aim, main control parameters, such as MFB_{50} and A/F

ratio are compared in Fig. 2. As before, the figure collects both *EIVC* and *Throttled* operating conditions, plotted in red and black colors, respectively.

A quite satisfactory agreement can be observed with reference to the MFB_{50} (Fig. 2a). Larger discrepancies are mainly found at low loads, where the computed combustion phasing stays at the optimal value more frequently than experiments. This is also due to the fixed MFB_{50-opt} specification, while in the experiments a fine tuning of the latter parameter has been performed. This, however, has a small impact on the computed BSFC. At medium-high loads, indeed, where a knock-related combustion phasing delay has to be imposed, the agreement is quite satisfactory, thanks to the accuracy of the employed knock model. A less satisfactory correlation is observed on estimated and measured A/F ratios in Fig. 2b. Actually, most of collected points are located close to the stoichiometric level, while richer and richer mixture qualities are required at high load and engine speed, for TIT control. The disagreement partly depends on inaccuracies in TIT prediction, already shown in Fig. 1c, but they are also due to some “security margins” probably included in the manufacturer calibration. Additional errors are related, for example, to the model overestimation of the in-cylinder mixture cooling due to fuel evaporation. The superimposed effects of overall calibration strategy and model accuracy can be appreciated in BSFC comparisons reported in Fig. 2c. Most of points are included in a $\pm 5\%$ error band. The few ones out of the above band are the same presenting high A/F ratio errors.

A quite good overall accuracy of both 1D model and calibration strategy is hence demonstrated, thus allowing the employment of this procedure to compute the entire engine map for both *EIVC* and *Throttled* modes.

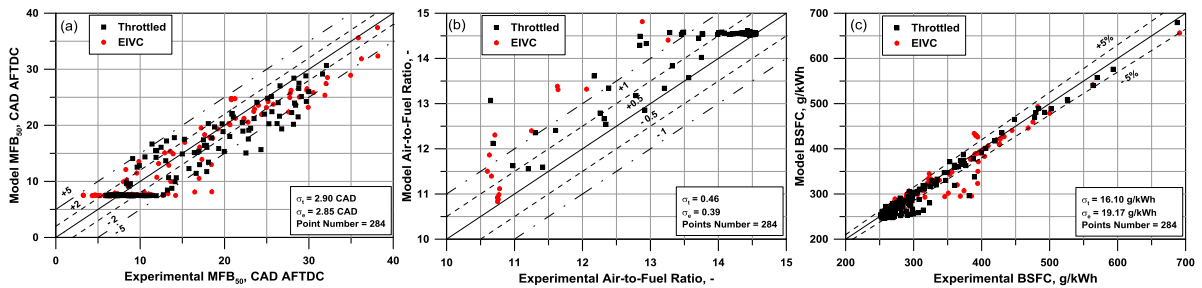


Fig. 2. Experimental vs Model MFB_{50} (a), A/F ratio (b), and BSFC (c)

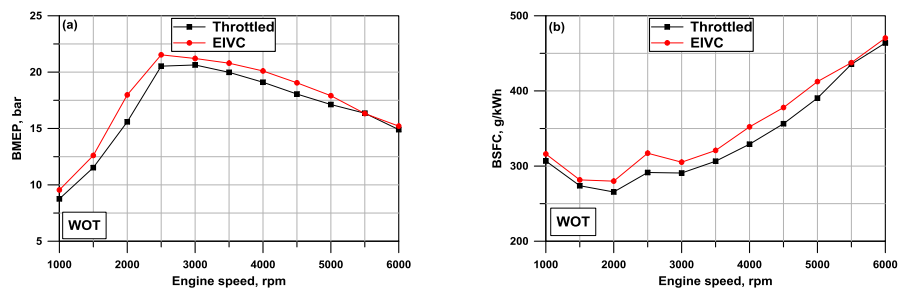


Fig. 3. BMEP vs engine speed (a), BSFC vs engine speed (b) for *Throttled* and *EIVC* strategies at full load

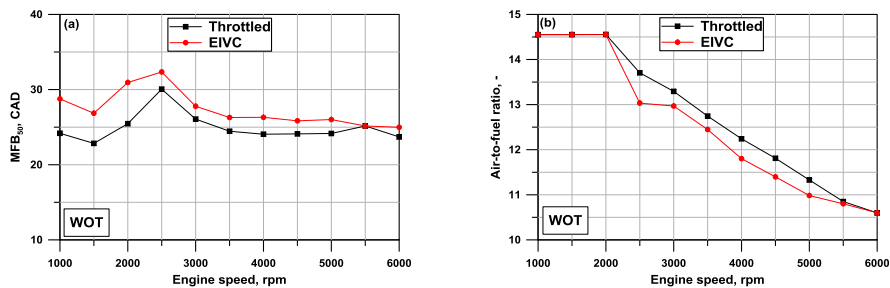


Fig. 4. MFB_{50} vs engine speed (a), Air-to-fuel ratio vs engine speed (b) for *Throttled* and *EIVC* strategies at full load

Fig. 3 and Fig. 4 report the full load results for the examined engine control strategies. In Fig. 3a, *EIVC* strategy shows BMEP improvements with respect to *Throttled* one in the whole speed range (except for higher speeds), mainly thanks to a higher volumetric efficiency related to the selected IVC for each speed. Fig. 3b highlights that a higher BSFC is obtained for *EIVC* approach at full load. Indeed, knock avoidance requires a more delayed combustion phasing for *EIVC* solution with respect to *Throttled* one (Fig. 4a). Consequently, a richer A/F ratio is selected by the calibration strategy for *EIVC* case (Fig. 4b).

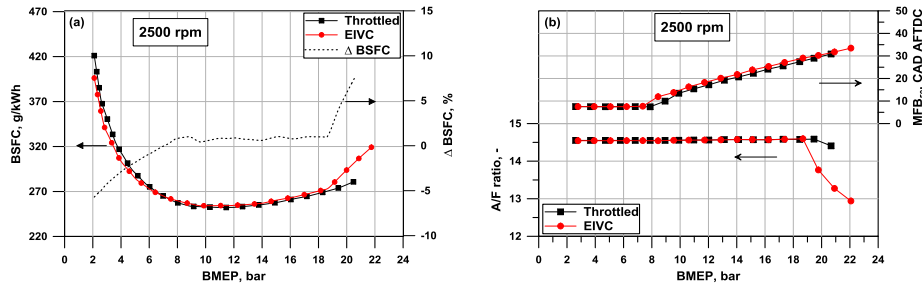


Fig. 5. BSFC vs BMEP (a), MFB₅₀ and A/F ratio vs BMEP (b) for an engine speed of 2500 rpm

BSFC, MFB₅₀ and A/F ratio trends with load level are shown in Fig. 5 at a reference speed of 2500 rpm, for both control approaches. As expected, BSFC benefits for *EIVC* strategy are obtained up to a BMEP level of about 7 bar (Fig. 5a), due to a reduced pumping losses. A maximum advantage of 6% is estimated at the lowest load level. Above 7 bar BMEP, on the contrary, the defined *EIVC* strategy, aiming to maximize the volumetric efficiency, involves a slightly more delayed combustion phasing than *Throttled* operation, together with a more relevant mixture over-fuelling at high loads for TIT control (Fig. 5b). Consistently, BSFC penalties are now obtained, as better quantified by the Δ BSFC trend reported in Fig. 5a (dashed line). Of course, a more aggressive calibration policy may be also defined, by a different selection of IVC at each load level, aiming to reduce the knock tendency. An earlier valve closure, in fact, while reducing the power output, would involve the well-known “syringe effect”, which reduces the mixture temperature at the end of the compression strokes, with some benefits on knock tendency.

A complete representation of the engine behavior is reported in Fig. 6, showing the BSFC maps both for *Throttled* and *EIVC* strategies, together with the related Δ BSFC map. BSFC benefits of *EIVC* strategy are ensured at low loads for various speeds, while some BSFC penalization occurs at high loads, especially at 2500–3000 rpm. The presented procedure allows to obtain a reliable first-attempt engine calibration, which may be further refined at the test bench with a reduced set of experimental tests, thus allowing for reduced time and costs of engine development phase.

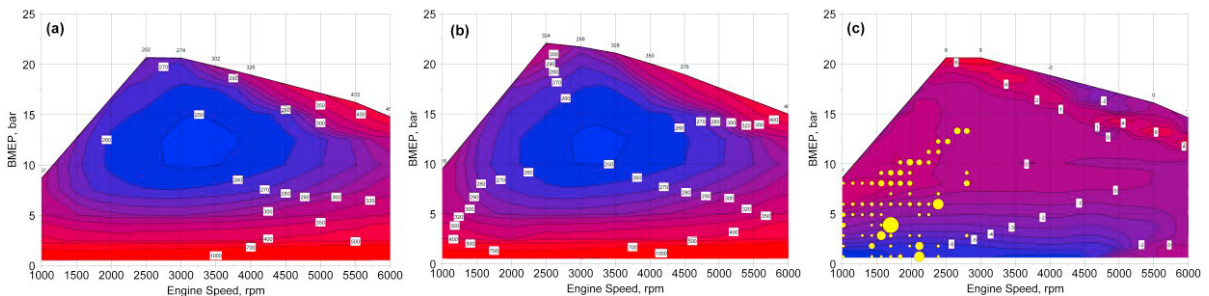


Fig. 6. BSFC maps for *Throttled* strategy (a) and for *EIVC* strategy (b); percent Δ BSFC map with fuel consumption bubble chart (c).

4. Vehicle Simulation: results discussion

A further result of the discussed calibration procedure is the possibility to also apply the computed maps in a vehicle simulation model, to quantify the CO₂ emission over a New European Driving Cycle (NEDC). In this way, various

control strategies can be also numerically compared early during the development phase of a new engine. This simulation is developed in AmesimTM environment, where a reference vehicle of segment A is schematized, while the engine is described by a quasi-steady map based approach. The simulation executes a so-called “backward kinematic analysis”, where, at each simulation step, the instantaneous engine operating point is identified based on the tractive demand required by the vehicle to follow the imposed speed profile. The gear shift strategy is imposed by the Regulation n.83 (United Nations Economic Commission for Europe) for vehicles with manual transmission [13]. More details on vehicle model and data can be found in [11]. Results of this analysis are superimposed on Δ BSFC map displayed in Fig. 6c. Bubbles size in the figure is proportional to the local fuel consumed along the NEDC. As shown, related operating points are mainly located in the low speed – low load region, where the *EIVC* strategy allows for maximum BSFC improvements. The overall fuel consumption is of 4.50 and 4.58 l/100km, for *EIVC* and *Throttled* strategies, respectively, corresponding to 102.1 and 103.6 gCO₂/km. As expected, the *EIVC* strategy guarantees some fuel rate and CO₂ reduction (about 1.9% and 1.4%, respectively). Of course, the above results may change if a different driving cycle is analyzed, such as the WLTP one, where a more frequent high load engine operation is required.

5. Conclusions

This paper proposes a virtual calibration methodology to automatically identify the control parameters for optimal performance of a downsized VVA SI engine in entire operating plane. 1D engine model is coupled to phenomenological sub-models for in-cylinder phenomena description and is validated against experimental findings, acquired in different speed/load points and control strategies (*EIVC* and *Throttled*). A numerical calibration procedure is proposed able to automatically identify the optimal set of calibration parameters all over the operating plane, considering various constraints for engine and sub-components safety.

Following the above procedure, engine maps are computed for both *EIVC* and *Throttled* strategies. Results underlined that *EIVC* strategy allows for BSFC benefits (max 6%) at part load (up to about 7 bar BMEP) and Torque improvements (max 15.3% at 2000 rpm) at full load with respect to the *Throttled* one.

The employment of computed maps in a vehicle model highlights that *EIVC* solution allows for a 1.9% reduction of the fuel rate and 1.4% reduction of CO₂ emission along a NEDC driving cycle.

Summarizing, the proposed numerical procedure, based on a validated 1D model enhanced by phenomenological sub-models, showed the potential to support the engine calibration, reducing the engine development costs and time.

References

- [1] Roepke K., Fisher M. (2001) “Efficient layout and calibration of variable valve trains”, SAE Technical Paper 2001-01-0688.
- [2] Grasreiner S., Neumann J., Wensing M., Hasse C. (2017) “Model-based virtual engine calibration with the help of phenomenological methods for spark-ignited engines”, Appl. Therm. Eng. 131 (2017) 190-199.
- [3] Bozza F., De Bellis V., Teodosio L. (2016) “A numerical procedure for the calibration of a turbocharged spark-ignition variable valve actuation engine at part load”, Int. Journal of Engine Research, October 2016, doi: 10.1177/1468087416674653.
- [4] Gouldin F. (2005) “An application of fractals to modeling premixed turbulent flames”, Comb.&Flame 68(3):249–66, 1987,
- [5] Bozza F., Gimelli A., Merola S., Vaglieco B. “Validation of a Fractal Combustion Model through Flame Imaging”, SAE 2005-01-1120.
- [6] Rhodes D, Keck J, (1985) “Laminar burning speed measurements of indolene-air-diluent mixtures at high pressures and temperatures”, SAE paper 850047, doi:10.4271/850047.
- [7] Bozza F., De Bellis V., Tufano D. “A comparison between two phenomenological combustion models for SI engines”, SAE 2017-01-2184.
- [8] Matthews R. D., Chin Y. W., “A Fractal-Based SI Engine Model: Comparisons of Predictions with Experimental Data”, SAE Paper 910075.
- [9] Andrae J. (2013) “Comprehensive chemical kinetic modeling of toluene reference fuels oxidation”, Fuel 2013; 107:740–8.
- [10] Bozza F., De Bellis V., Teodosio L., (2016) “Potentials of cooled EGR and water injection for knock resistance and fuel consumption improvements of gasoline engines”, Applied Energy 169: 112–125, 2016, doi: 10.1016/j.apenergy.2016.01.129.
- [11] Teodosio L., Bozza F., De Bellis V., Tufano D. (2017) “Numerical Study of the Potential of a Variable Compression Ratio Concept applied to Downsized Turbocharged VVA Spark Ignition engine”, SAE Technical Paper 2017-24-0015, doi: 10.4271/2017-24-0015.
- [12] Bozza F., De Bellis V., Teodosio L., Gimelli A., “Numerical analysis of the transient operation of a turbocharged diesel engine including the compressor surge”, Proc. of the Inst. of Mech. Eng., Part D, J. of Automobile Engineering, Vol. 227, (11), pp. 1503-1517, 2013, doi:10.1177/0954407013501668.
- [13] Official Journal of UE, “Regulation N. 83 of the Economic Commission for Europe of the United Nations (UN/ECE) – Uniform provisions concerning the approval of vehicles with regard to the emission of pollutants according to engine fuel requirements”, L 375/223, 2006.